An axisymmetric heat conduction model for a multi-material cylindrical system with application to analysis of carbon nanotube based composites

Whye-Teong Ang

School of Mechanical and Aerospace Engineering
Nanyang Technological University
50 Nanyang Avenue, Singapore 639798

Indra Vir Singh and Masataka Tanaka
Department of Mechanical Systems Engineering
Faculty of Engineering, Shinshu University
Nagano 380-8553, Japan

Abstract

A model for axisymmetric steady-state heat conduction in a multi-material cylindrical system containing a thermal superconductor is presented. An analytical solution in terms of series involving Bessel functions is derived for the temperature distribution in the multi-material system. The model may be applied to analyze the thermal behaviors of carbon nanotube based composites. Some results are obtained for specific cases of the multi-material system.

1 Introduction

Heat conduction in cylindrical solid systems has important applications in many areas of modern engineering, such as in thermal analysis of computer chips and carbon nanotubes. Because of this, it has attracted the attention of many researchers. For example, Kennedy (1960) obtained a series solution in terms of Bessel functions for the temperature in a homogeneous cylinder and applied it to derive a formula for the spreading resistance in semi-conductor devices, and Hui and Tan (1994) employed Dini series and Hankel transform to find the temperature distribution in a cylindrical head spreader bonded to a semi-infinite heat sink. More recently, Desai, Geer and Sammakia (2006) presented an analytical model for the axisymmetric steady-state heat conduction in three contiguous dissimilar co-axial cylindrical solids of different radii and showed how it could be used for analyzing thermal management systems in electronic packaging. More references on the analysis of heat conduction in cylindrical systems may be found in the papers cited above.

In the present paper, a model for axisymmetric steady-state heat conduction in a multi-material cylindrical system containing a thermal superconductor is presented. The cylindrical system, as sketched in Figure 1, is made up of three dissimilar materials in the regions denoted by R_1, R_2 and R_3. The interfaces between the materials are perfectly bonded. A uniform temperature is prescribed on each of the flat ends of the multi-material cylinder. The curved part of the exterior boundary of the cylinder is thermally insulated. The surface temperature of the thermal superconductor is taken to be an unknown constant to be determined. The total heat energy flowing across the surface of the thermal superconductor is specified as zero.

An analytical solution is derived for the model in terms of series containing Bessel functions. The coefficients of the truncated series are determined by solving a system of linear algebraic equations. The solution is applied to examine a few specific cases of the model. A particular case of interest concerns the thermal analysis of a carbon nanotube based composite, such as the calculation of the equivalent (effective) thermal conductivity of a cylindrical representative volume element containing a carbon nanotube.

2 Mathematical statement of the model

With reference to an $Oxyz$ Cartesian coordinate system, the multi-material cylindrical system under consideration here comprises the regions R_1, R_2 and R_3 given by

$$
\begin{aligned}
R_1 &= \{(x,y,z): \ x^2+y^2 < r_2^2, \ 0 < z < \ell_1\}, \\
R_2 &= \{(x,y,z): \ r_1^2 < \ x^2+y^2 < r_2^2, \ \ell_1 < z < \ell_2\}, \\
R_3 &= \{(x,y,z): \ x^2+y^2 < r_2^2, \ \ell_2 < z < \ \ell_3\}.
\end{aligned}
\tag{1}
$$

The regions R_1, R_2 and R_3 are occupied by possibly dissimilar thermally isotropic and homogeneous materials with thermal conductivities k_1, k_2 and k_3 respectively. The region $x^2 + y^2 < r_1^2$, $\ell_1 < z < \ell_2$, is occupied by a thermal superconductor. Refer to Figure 1.
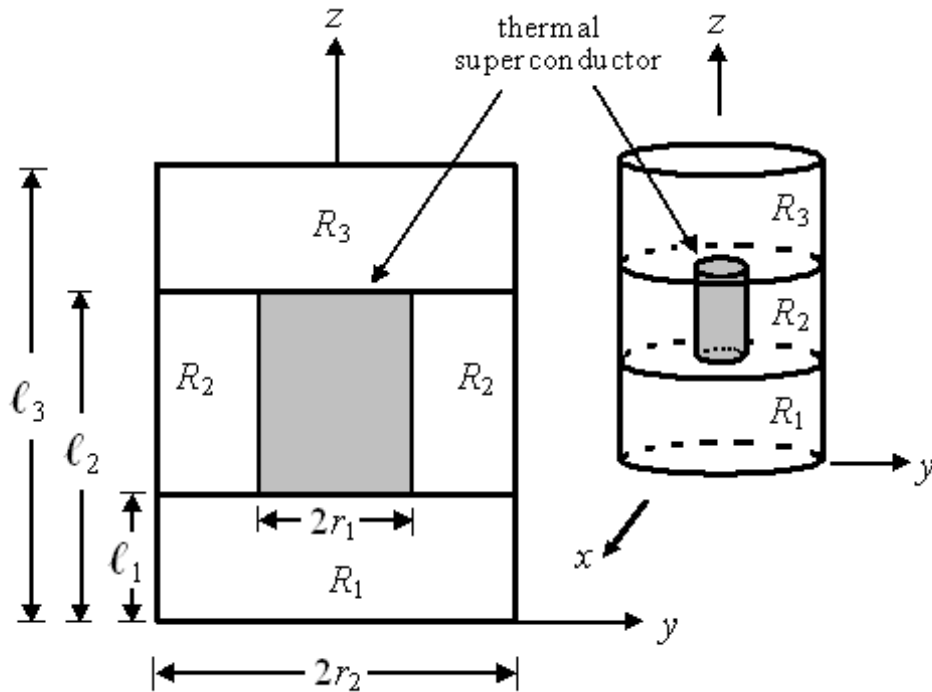

Figure 1. Geometrical sketches of the multi-material cylindrical system.

The temperature in the multi-material cylindrical system is assumed to be dependent on the coordinates r and z only. Here r is the perpendicular distance of the point (x, y, z) from the z axis, that is, $r = \sqrt{x^2 + y^2}$. Let the temperature in R_i be given by $T_i(r, z)$. The temperature T_i is required to satisfy the Laplace's equation in R_i, that is,

$$\frac{\partial^2 T_i}{\partial r^2} + \frac{1}{r}\frac{\partial T_i}{\partial r} + \frac{\partial^2 T_i}{\partial z^2} = 0 \text{ in } R_i \ (i = 1, 2, 3). \tag{2}$$

The interfaces between the dissimilar materials are assumed to be perfectly bonded so that

$$\left.\begin{aligned} T_2(r, \ell_1) &= T_1(r, \ell_1) \\ T_2(r, \ell_2) &= T_3(r, \ell_2) \\ k_2 \left.(\partial T_2/\partial z)\right|_{z=\ell_1} &= k_1 \left.(\partial T_1/\partial z)\right|_{z=\ell_1} \\ k_2 \left.(\partial T_2/\partial z)\right|_{z=\ell_2} &= k_3 \left.(\partial T_3/\partial z)\right|_{z=\ell_2} \end{aligned}\right\} \text{ for } r_1 < r < r_2. \tag{3}$$

The temperature is taken to be a yet to be determined constant T_{sc} on the surface S of the thermal superconductor, that is,

$$T_1(r, \ell_1) = T_{\text{sc}} \text{ for } 0 \le r < r_1, \tag{4}$$

$$T_2(r_1, z) = T_{\text{sc}} \text{ for } \ell_1 < z < \ell_2, \tag{5}$$

$$T_3(r, \ell_2) = T_{\text{sc}} \text{ for } 0 \le r < r_1, \tag{6}$$

Furthermore, it is required that

$$k_2 r_1 \int_{\ell_1}^{\ell_2} \left.\frac{\partial T_2}{\partial r}\right|_{r=r_1} dz + \int_0^{r_1} \left(k_3 \left.\frac{\partial T_3}{\partial z}\right|_{z=\ell_2} - k_1 \left.\frac{\partial T_1}{\partial z}\right|_{z=\ell_1}\right) r \, dr = 0. \tag{7}$$

Note that (7) states that the total heat energy flowing across the surface S into the thermal superconductor is zero.

The conditions on the outer boundary of the multi-material cylindrical system are given by

$$\left.\begin{aligned} T_1(r, 0) &= T_{\text{bottom}} \\ T_3(r, \ell_3) &= T_{\text{top}} \end{aligned}\right\} \text{ for } 0 \le r < r_2, \tag{8}$$

and

$$\left.\frac{\partial T_i}{\partial r}\right|_{r=r_2} = 0 \text{ for } \ell_{i-1} < z < \ell_i \ (i = 1, 2, 3), \tag{9}$$

4

where $\ell_0 = 0$ and T_{bottom} and T_{top} are suitably prescribed constants. According to (8), the temperature is a constant on each of the flat ends of the cylinder. The condition in (9) implies that the curved part of the outer boundary is thermally insulated.

The temperature distribution in the multi-material cylindrical system (with the thermal superconductor) is determined by solving (2) subject to (3)-(9).

3 Analytical solution of the model

Through application of the method of separation of variables on (2) together with (5), (8) and (9), one finds that T_1, T_2 and T_3 may be written as

$$
\begin{aligned}
T_1(r,z) &= T_{\text{bottom}} + a_0 \frac{z}{r_2} + \sum_{n=1}^{\infty} a_n J_0(j_{1,n} \frac{r}{r_2}) \sinh(j_{1,n} \frac{z}{r_2}), \\
T_2(r,z) &= T_{\text{sc}} + \sum_{n=1}^{\infty} [J_0(\sigma_n \frac{r}{r_2}) - \frac{J_0(\sigma_n r_1/r_2)}{Y_0(\sigma_n r_1/r_2)} Y_0(\sigma_n \frac{r}{r_2})] \\
&\quad \times [b_n \cosh(\frac{\sigma_n}{r_2}[z - \frac{1}{2}(\ell_1 + \ell_2)]) + c_n \sinh(\frac{\sigma_n}{r_2}[z - \frac{1}{2}(\ell_1 + \ell_2)])], \\
T_3(r,z) &= T_{\text{top}} + d_0 \frac{(z - \ell_3)}{r_2} + \sum_{n=1}^{\infty} d_n J_0(j_{1,n} \frac{r}{r_2}) \sinh(j_{1,n} \frac{(z - \ell_3)}{r_2}), \quad (10)
\end{aligned}
$$

where J_0 and Y_0 are the zeroth order Bessel functions of the first and the second kinds respectively, a_0, d_0, a_n, b_n, c_n and d_n ($n = 1, 2, \cdots$) are real constant coefficients yet to the determined, $j_{1,n}$ are the zeroes of the first order Bessel function of the first kind, that is, $J_1(j_{1,n}) = 0$ and $j_{1,n} < j_{1,n+1}$ for $n = 1, 2, \cdots$, and σ_n are such that $J_0(\sigma_n r_1/r_2) Y_1(\sigma_n) - Y_0(\sigma_n r_1/r_2) J_1(\sigma_n) = 0$ and $\sigma_n < \sigma_{n+1}$ for $n = 1, 2, \cdots$.

Now the first line in (3) and (4) may be collectively written as

$$
T_1(r, \ell_1) = \begin{cases} T_{\text{sc}} & \text{for} \quad 0 \le r < r_1, \\ T_2(r, \ell_1) & \text{for} \quad r_1 < r < r_2. \end{cases} \quad (11)
$$

If (11) is multiplied by r and then integrated over the interval $0 \le r \le r_2$,

one obtains

$$\frac{1}{2}(T_{\text{bottom}} + a_0\frac{\ell_1}{r_2} - T_{\text{sc}})r_2^2$$

$$= \sum_{n=1}^{\infty} A_{0n}[b_n \cosh(\frac{\sigma_n}{2r_2}[\ell_2 - \ell_1]) - c_n \sinh(\frac{\sigma_n}{2r_2}[\ell_2 - \ell_1])], \qquad (12)$$

where

$$A_{0n} = \int_{r_1}^{r_2} r[J_0(\sigma_n\frac{r}{r_2}) - \frac{J_0(\sigma_n r_1/r_2)}{Y_0(\sigma_n r_1/r_2)}Y_0(\sigma_n\frac{r}{r_2})]dr$$

$$= \frac{r_1 r_2}{\sigma_n Y_0(\sigma_n r_1/r_2)}[J_0(\sigma_n\frac{r_1}{r_2})Y_1(\sigma_n\frac{r_1}{r_2}) - Y_0(\sigma_n\frac{r_1}{r_2})J_1(\sigma_n\frac{r_1}{r_2})]$$

$$\text{for } n = 1, 2, \cdots. \qquad (13)$$

Note that T_{sc} is an unknown constant to be determined.

Integrating (11) multiplied by $rJ_0(j_{1,m}r/r_2)$ ($m = 1, 2, \cdots$) over $0 \le r \le r_2$ yields

$$\frac{1}{2}a_m r_2^2 \sinh(j_{1,m}\frac{\ell_1}{r_2})(J_0(j_{1,m}))^2$$

$$= \sum_{n=1}^{\infty} A_{mn}[b_n \cosh(\frac{\sigma_n}{2r_2}[\ell_2 - \ell_1]) - c_n \sinh(\frac{\sigma_n}{2r_2}[\ell_2 - \ell_1])]$$

$$\text{for } m = 1, 2, \cdots. \qquad (14)$$

where

$$A_{mn} = \int_{r_1}^{r_2} r[J_0(\sigma_n\frac{r}{r_2}) - \frac{J_0(\sigma_n r_1/r_2)}{Y_0(\sigma_n r_1/r_2)}Y_0(\sigma_n\frac{r}{r_2})]J_0(j_{1,m}\frac{r}{r_2})dr$$

$$= \frac{r_2}{j_{1,m}^2 - \sigma_n^2}[-r_2\sigma_n J_0(j_{1,m})J_1(\sigma_n) + r_1\sigma_n J_0(j_{1,m}\frac{r_1}{r_2})J_1(\sigma_n\frac{r_1}{r_2})$$

$$-r_1 j_{1,m}J_1(j_{1,m}\frac{r_1}{r_2})J_0(\sigma_n\frac{r_1}{r_2}) - \frac{J_0(\sigma_n r_1/r_2)}{Y_0(\sigma_n r_1/r_2)}\{-r_2\sigma_n J_0(j_{1,m})Y_1(\sigma_n)$$

$$+r_1\sigma_n J_0(j_{1,m}\frac{r_1}{r_2})Y_1(\sigma_n\frac{r_1}{r_2}) - r_1 j_{1,m}J_1(j_{1,m}\frac{r_1}{r_2})Y_0(\sigma_n\frac{r_1}{r_2})\}]$$

$$\text{for } m, n = 1, 2, \cdots. \qquad (15)$$

6

Similarly, the second line of (3) and (6) may be applied to obtain

$$\frac{1}{2}(T_{\text{top}} + \frac{d_0(\ell_2 - \ell_3)}{r_2} - T_{\text{sc}})r_2^2$$

$$= \sum_{n=1}^{\infty} A_{0n}[b_n \cosh(\frac{\sigma_n}{2r_2}[\ell_2 - \ell_1]) + c_n \sinh(\frac{\sigma_n}{2r_2}[\ell_2 - \ell_1])], \qquad (16)$$

and

$$\frac{1}{2}d_m r_2^2 \sinh(j_{1,m}\frac{[\ell_2 - \ell_3]}{r_2})(J_0(j_{1,m}))^2$$

$$= \sum_{n=1}^{\infty} A_{mn}[b_n \cosh(\frac{\sigma_n}{2r_2}[\ell_2 - \ell_1]) + c_n \sinh(\frac{\sigma_n}{2r_2}[\ell_2 - \ell_1])]$$

$$\text{for } m = 1, 2, \cdots . \qquad (17)$$

To treat the condition on the third line of (3), a yet to be determined function $Q_1(r)$ is introduced to represent the unknown heat flux flowing out of the thermal superconductor through the surface $0 \le r < r_1$, $z = \ell_1$. As the temperature is a constant at all points on the surface of the thermal superconductor, one may expect $Q_1(r_1) = 0$ and take $Q_1(r)$ to be in the series form

$$Q_1(r) = \sum_{n=1}^{\infty} f_n J_0(j_{0,n}\frac{r}{r_1}), \qquad (18)$$

where f_n are real constant coefficients to be determined and $j_{0,n}$ are the zeroes of the zeroth order Bessel function of the first kind, that is, $J_0(j_{0,n}) = 0$ and $j_{0,n} < j_{0,n+1}$ for $n = 1, 2, \cdots$.

The condition on the third line of (3) may now be written as:

$$k_1 (\partial T_1/\partial z)|_{z=\ell_1} = \begin{cases} Q_1(r) & \text{for } 0 \le r < r_1, \\ k_2 (\partial T_2/\partial z)|_{z=\ell_1} & \text{for } r_1 < r < r_2. \end{cases} \qquad (19)$$

If one proceeds in a similar manner as in the derivation of (12), (14), (16) and (17), one finds that (19) gives rise to

$$\frac{1}{2}k_1 a_0 r_2 = \sum_{n=1}^{\infty} \frac{1}{r_2}k_2 A_{0n}\sigma_n[-b_n \sinh(\frac{\sigma_n}{2r_2}[\ell_2 - \ell_1]) + c_n \cosh(\frac{\sigma_n}{2r_2}[\ell_2 - \ell_1])]$$

$$+ r_1^2 \sum_{n=1}^{\infty} \frac{f_n}{j_{0,n}} J_1(j_{0,n}) \qquad (20)$$

7

and

$$\frac{1}{2}k_1 j_{1,m} a_m r_2 \cosh(j_{1,m}\frac{\ell_1}{r_2})[J_0(j_{1,m})]^2$$

$$= \sum_{n=1}^{\infty} \frac{f_n j_{0,n} J_1(j_{0,n}) J_0(j_{1,m} r_1/r_2)}{(j_{0,n}/r_1)^2 - (j_{1,m}/r_2)^2}$$

$$+ \sum_{n=1}^{\infty} \frac{1}{r_2} k_2 A_{mn} \sigma_n [-b_n \sinh(\frac{\sigma_n}{2r_2}[\ell_2 - \ell_1]) + c_n \cosh(\frac{\sigma_n}{2r_2}[\ell_2 - \ell_1])]$$

$$\text{for } m = 1, 2, \cdots. \tag{21}$$

For the last condition in (3), the unknown function $Q_2(r)$ representing the heat flux flowing into the thermal superconductor through the surface $0 \leq r < r_1$, $z = \ell_2$, is written in the series form

$$Q_2(r) = \sum_{n=1}^{\infty} g_n J_0(j_{0,n}\frac{r}{r_1}), \tag{22}$$

where g_n are constant coefficients to be determined.

It follows that

$$\frac{1}{2}k_3 d_0 r_2 = \sum_{n=1}^{\infty} \frac{1}{r_2} k_2 A_{0n} \sigma_n [b_n \sinh(\frac{\sigma_n}{2r_2}[\ell_2 - \ell_1]) + c_n \cosh(\frac{\sigma_n}{2r_2}[\ell_2 - \ell_1])]$$

$$+ r_1^2 \sum_{n=1}^{\infty} \frac{g_n}{j_{0,n}} J_1(j_{0,n}) \tag{23}$$

and

$$\frac{1}{2}k_3 j_{1,m} d_m r_2 \cosh(j_{1,m}\frac{[\ell_2 - \ell_3]}{r_2})[J_0(j_{1,m})]^2$$

$$= \sum_{n=1}^{\infty} \frac{g_n j_{0,n} J_1(j_{0,n}) J_0(j_{1,m} r_1/r_2)}{(j_{0,n}/r_1)^2 - (j_{1,m}/r_2)^2}$$

$$+ \sum_{n=1}^{\infty} \frac{1}{r_2} k_2 A_{mn} \sigma_n [b_n \sinh(\frac{\sigma_n}{2r_2}[\ell_2 - \ell_1]) + c_n \cosh(\frac{\sigma_n}{2r_2}[\ell_2 - \ell_1])]$$

$$\text{for } m = 1, 2, \cdots. \tag{24}$$

8

Lastly, the condition in (7) gives rise to

$$
2k_2 r_1 \sum_{n=1}^{\infty} [-J_1(\sigma_n \frac{r_1}{r_2}) + \frac{J_0(\sigma_n r_1/r_2)}{Y_0(\sigma_n r_1/r_2)} Y_1(\sigma_n \frac{r_1}{r_2})] b_n \sinh(\frac{\sigma_n}{2r_2}[\ell_2 - \ell_1])
$$

$$
+ \sum_{n=1}^{\infty} (g_n - f_n) \frac{r_1^2}{j_{0,n}} J_1(j_{0,n})
$$

$$
= 0 \tag{25}
$$

To summarize, the temperature distribution in the multi-material cylindrical system is given by (10) together with (12), (14), (16), (17), (20), (21), (23), (24) and (25).

For the purpose of practical computation, all the series above must be truncated. This may be done by replacing ∞ in the series by a finite but sufficiently large integer N_∞. Firstly, the required unknown constants T_{sc}, b_n, c_n, f_n and g_n ($n = 1, 2, \cdots, N_\infty$) are determined by solving the truncated form of (25) (with ∞ replaced by N_∞ in the series), that is,

$$
2 \sum_{n=1}^{N_\infty} [-J_1(\sigma_n \frac{r_1}{r_2}) + \frac{J_0(\sigma_n r_1/r_2)}{Y_0(\sigma_n r_1/r_2)} Y_1(\sigma_n \frac{r_1}{r_2})] b_n \sinh(\frac{\sigma_n}{2r_2}[\ell_2 - \ell_1])
$$

$$
+ \sum_{n=1}^{N_\infty} \frac{r_1}{k_2} (g_n - f_n) \frac{J_1(j_{0,n})}{j_{0,n}}
$$

$$
= 0 \tag{26}
$$

together with

$$
\sum_{n=1}^{N_\infty} \frac{A_{0n}}{r_2^2} [b_n(\cosh(\frac{\sigma_n}{2r_2}[\ell_2 - \ell_1]) + \frac{k_2 \ell_1 \sigma_n}{k_1 r_2} \sinh(\frac{\sigma_n}{2r_2}[\ell_2 - \ell_1]))
$$

$$
+ c_n(- \sinh(\frac{\sigma_n}{2r_2}[\ell_2 - \ell_1]) - \frac{k_2 \ell_1 \sigma_n}{k_1 r_2} \cosh(\frac{\sigma_n}{2r_2}[\ell_2 - \ell_1]))]
$$

$$
- \frac{\ell_1 r_1^2}{k_1 r_2^2} \sum_{n=1}^{N_\infty} \frac{f_n}{j_{0,n}} J_1(j_{0,n}) + \frac{1}{2} T_{sc}
$$

$$
= \frac{1}{2} T_{\text{bottom}}, \tag{27}
$$

9

$$
\sum_{n=1}^{N_\infty} \frac{A_{mn}}{r_2^2} [b_n \cosh(\frac{\sigma_n}{2r_2}[\ell_2 - \ell_1]) - c_n \sinh(\frac{\sigma_n}{2r_2}[\ell_2 - \ell_1])]
$$

$$
- \sum_{n=1}^{N_\infty} \frac{k_2 \sigma_n A_{mn} \sinh(j_{1,m}\ell_1/r_2)}{r_2^2 k_1 j_{1,m} \cosh(j_{1,m}\ell_1/r_2)}
$$

$$
\times [-b_n \sinh(\frac{\sigma_n}{2r_2}[\ell_2 - \ell_1]) + c_n \cosh(\frac{\sigma_n}{2r_2}[\ell_2 - \ell_1])]
$$

$$
- \sum_{n=1}^{N_\infty} \frac{f_n j_{0,n} J_1(j_{0,n}) J_0(j_{1,m}r_1/r_2) \sinh(j_{1,m}\ell_1/r_2)}{k_1 j_{1,m}[(j_{0,n}/r_1)^2 - (j_{1,m}/r_2)^2] r_2 \cosh(j_{1,m}\ell_1/r_2)}
$$

$$
= \quad 0 \quad \text{for } m = 1, 2, \cdots, 2N_\infty - 1, \tag{28}
$$

$$
\sum_{n=1}^{N_\infty} \frac{A_{0n}}{r_2^2} [b_n (\cosh(\frac{\sigma_n}{2r_2}[\ell_2 - \ell_1]) - \frac{(\ell_2 - \ell_3)k_2\sigma_n}{k_3 r_2} \sinh(\frac{\sigma_n}{2r_2}[\ell_2 - \ell_1]))
$$

$$
+ c_n (\sinh(\frac{\sigma_n}{2r_2}[\ell_2 - \ell_1]) - \frac{(\ell_2 - \ell_3)k_2\sigma_n}{k_3 r_2} \cosh(\frac{\sigma_n}{2r_2}[\ell_2 - \ell_1]))]
$$

$$
- \frac{(\ell_2 - \ell_3)r_1^2}{k_3 r_2^2} \sum_{n=1}^{N_\infty} \frac{g_n}{j_{0,n}} J_1(j_{0,n}) + \frac{1}{2} T_{\text{sc}}
$$

$$
= \quad \frac{1}{2} T_{\text{top}}, \tag{29}
$$

and

$$
\sum_{n=1}^{N_\infty} \frac{A_{mn}}{r_2^2} [b_n \cosh(\frac{\sigma_n}{2r_2}[\ell_2 - \ell_1]) + c_n \sinh(\frac{\sigma_n}{2r_2}[\ell_2 - \ell_1])]
$$

$$
- \sum_{n=1}^{N_\infty} \frac{k_2 \sigma_n A_{mn} \sinh(j_{1,m}[\ell_2 - \ell_3]/r_2)}{r_2^2 k_3 j_{1,m} \cosh(j_{1,m}[\ell_2 - \ell_3]/r_2)}
$$

$$
\times [b_n \sinh(\frac{\sigma_n}{2r_2}[\ell_2 - \ell_1]) + c_n \cosh(\frac{\sigma_n}{2r_2}[\ell_2 - \ell_1])]
$$

$$
- \sum_{n=1}^{N_\infty} \frac{g_n j_{0,n} J_1(j_{0,n}) J_0(j_{1,m}r_1/r_2) \sinh(j_{1,m}[\ell_2 - \ell_3]/r_2)}{k_3 j_{1,m}[(j_{0,n}/r_1)^2 - (j_{1,m}/r_2)^2] r_2 \cosh(j_{1,m}[\ell_2 - \ell_3]/r_2)}
$$

$$
= \quad 0 \quad \text{for } m = 1, 2, \cdots, 2N_\infty - 1. \tag{30}
$$

Note that (27), (28), (29) and (30) are derived from (12), (14), (16), (17), (20), (21), (23), (24) by eliminating a_0, a_m, d_0 and d_m ($m = 1, 2, \cdots, N_\infty$).

The values of the constants $j_{0,n}$ $j_{1,n}$ and σ_n required for setting up (26), (27), (28), (29) and (30) may be easily obtained by using mathematical software packages such as Mathematica and Maple.

Once T_{sc}, $b_n \exp(\sigma_n[\ell_2 - \ell_1]/[2r_2])$, $c_n \exp(\sigma_n[\ell_2 - \ell_1]/[2r_2])$, f_n and g_n ($n = 1, 2, \cdots, N_\infty$) are determined from (26), (27), (28), (29) and (30), the other remaining unknown constants a_0, a_m, d_0 and d_m may then directly be computed from (12), (14), (16) and (17) ($m = 1, 2, \cdots, N_\infty$).

4   Carbon nanotube based composites

Carbon nanotubes are well known for their strongly enhanced properties such as high thermal conductivities (Iijima, 1991; and Berber, Kwon and Tomanék, 2000). In a recent work, Zhang, Tanaka and Matsumoto (2004) modeled a carbon nanotube as a thermal superconductor which has an unknown uniform temperature on its exterior surface boundary. For the steady-state heat conduction, the total heat energy flowing out of the superconductor (which models the carbon nanotube) into its embedding substrate is zero. Thus, the axisymmetric heat conduction model in Section 2 above may be applied to study the thermal behaviors of a carbon nanotube based composite.

If $k_1 = k_2 = k_3 = k$ and $\ell_1 + \ell_2 = \ell_3$ then the model may be regarded as a homogeneous cylindrical representative volume element containing a centrally located carbon nanotube, similar to the one considered in Singh, Tanaka and Endo (2006). The effective (equivalent) thermal conductivity k_{e} of the cylindrical representative volume element may be estimated using

$$k_{\text{e}} \simeq -\frac{q_{\text{ave}}\ell_3}{T_{\text{top}} - T_{\text{bottom}}}, \tag{31}$$

where q_{ave} is the average heat flux on the surface $0 \leq r < r_2$, $z = \ell_3$ given by

$$q_{\text{ave}} = -\frac{k}{\pi r_2^2} \int_0^{2\pi} \int_0^{r_2} \left.\frac{\partial T_3}{\partial z}\right|_{z=\ell_3} r\, dr\, d\theta = -\frac{kd_0}{r_2}. \tag{32}$$

Note that (32) is derived using the expression for T_3 in (10).

11

5 Specific cases

Case 1. The regions R_1, R_2 and R_3 are taken to be occupied by the same material elastomer S160 which has a thermal conductivity of 0.56 $\mathrm{Wm^{-1}K^{-1}}$ and are such that $\ell_1 + \ell_2 = \ell_3 = 100$ nm and $r_2 = 10$ nm. The temperature values T_bottom and T_top are taken to be 200 K and 100 K respectively. This case corresponds to the homogeneous cylindrical representative volume element containing a single carbon nanotube (mentioned in Section 4).

The effective thermal conductivity k_e of the representative volume element is computed using (31) and (32) with $N_\infty = 16$ for r_1 which is assigned the magnitudes 2.5, 5.0 and 7.5 nm and for selected values of $\ell = \ell_2 - \ell_1$ (the length of the carbon nanotube) over the interval $0 < \ell < 100$ (nm). When the calculation is repeated using $N_\infty = 32$, the value of k_e is found to converge to at least 2 significant figures. If ℓ is very small compared to the length of the representative volume element, convergence to 3 or even 4 significant figures may be observed.

For the purpose of comparison, numerical values of k_e are also obtained by using two different meshless techniques, namely the hybrid boundary node method and the element free Galerkin method. In applying the hybrid boundary node method for solving the three-dimensional Laplace's equation (as outlined in Zhang and Yao, 2001; Zhang, Yao and Li, 2002; and Zhang, Tanaka and Matsumoto, 2004), up to slightly over 10000 nodes are employed on the boundary of the solution domain (that is, on the outer boundary of the representative volume element and the interface between the carbon nanotube and the elastomer). The element free Galerkin method for axisymmetric heat conduction (see, for example, Singh, Tanaka and Endo, 2006) is used here with over 2000 nodes selectively distributed throughout the solution domain on the cross section $x = 0$.

In Table 1, the values of k_e computed using (31) and (32) with $N_\infty = 16$ for $r_1 = 5.0$ nm and some values of ℓ are compared with the numerical values calculated using the hybrid boundary node method and the two-dimensional element free Galerkin method. It is obvious that there is a reasonably good agreement between the three sets of values for k_e in Table 1.

Table 1. Values of k_e (in $\mathrm{Wm^{-1}K^{-1}}$) for $r_1 = 5$ nm and selected ℓ.

Length ℓ (in nm)	Formula (31)-(32)	Hybrid boundary node method	Element free Galerkin method
5	0.5754	0.5745	0.5781
10	0.6017	0.6007	0.6040
15	0.6343	0.6334	0.6310
20	0.6720	0.6709	0.6766
25	0.7147	0.7141	0.7201
30	0.7634	0.7621	0.7656
35	0.8193	0.8178	0.8222
40	0.8839	0.8823	0.8846
45	0.9597	0.9578	0.9660
50	1.050	1.048	1.058
55	1.158	1.156	1.164
60	1.292	1.289	1.299
65	1.460	1.457	1.467
70	1.679	1.675	1.682
75	1.975	1.970	1.979
80	2.398	2.391	2.421
85	3.052	3.042	3.064
90	4.205	4.189	4.211
95	6.927	6.894	6.930

In Figure 2, the value of k_e is plotted against ℓ over the interval $0 < \ell < 100$ (nm) for $r_1 = 2.5$, 5.0 and 7.5 nm. For a given ℓ, the effective thermal conductivity is observed to be greater in magnitude for a larger value of r_1. However, for small ℓ, the increase in k_e is only very slight as r_1 increases. The effect of increasing r_1 on k_e is more significant for ℓ which is closer 100 nm, that is, for a carbon nanotube whose length is comparable to the length of the representative volume element.
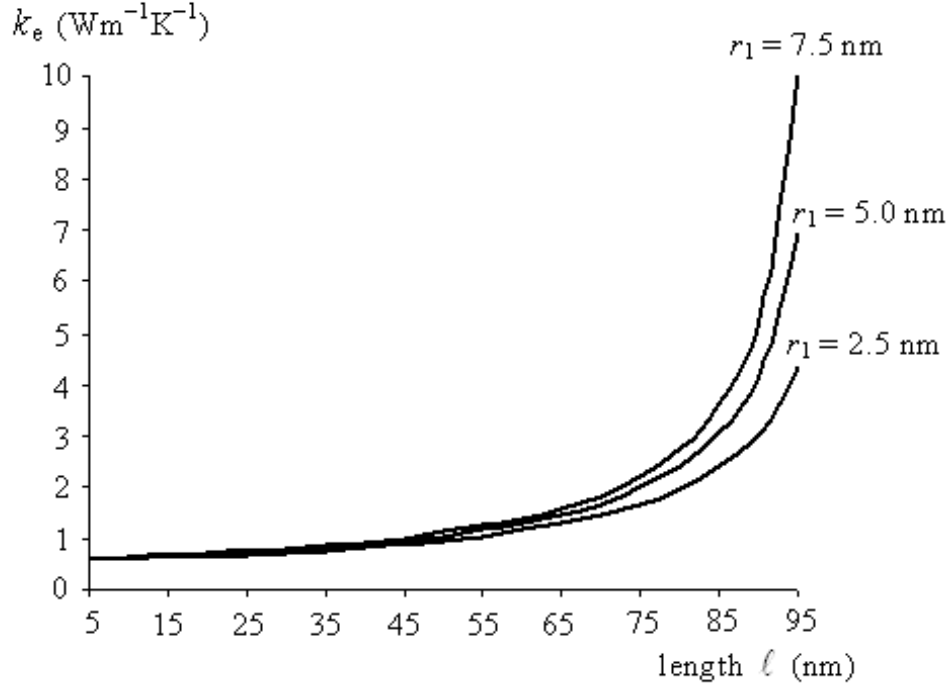
Figure 2. Plots of k_e against ℓ.

Case 2. Take R_1 and R_3 in Figure 1 to be occupied by silicon ($k_1 = 120$ $\mathrm{Wm^{-1}K^{-1}}$) and aluminium ($k_3 = 240$ $\mathrm{Wm^{-1}K^{-1}}$) respectively. The region R_2 is occupied by a thermal interface material of low thermal conductivity $k_2 = 1$ $\mathrm{Wm^{-1}K^{-1}}$. The lengths ℓ_1, ℓ_2 and ℓ_3 are taken to be 500, 510 and 1010 μm respectively, so that the silicon and the aluminium are separated from each other by a relatively thin layer of the thermal interface material. The radii r_1 and r_2 of the multi-material cylindrical system are respectively chosen to be 12.5 and 50 μm.

The curved part of the cylinder, that is, the surface $x^2 + y^2 = r_2^2$, $0 < z < \ell_3$, is thermally insulated. A constant heat flux $q_0 = 1000000$ $\mathrm{Wm^{-2}}$ enters the cylindrical system through the bottom surface of the cylinder $x^2 + y^2 < r_2^2$,

14

$z = 0$, that is,

$$k_1 \left.\frac{\partial T_1}{\partial z}\right|_{z=0} = -q_0 \quad \text{for } 0 \le r < r_2. \qquad (33)$$

Heat is removed by a convective process from the flat surface on top of the cylinder, that is,

$$k_3 \left.\frac{\partial T_3}{\partial z}\right|_{z=\ell_3} = -h[T_3(r, \ell_3) - T_{\text{amb}}] \quad \text{for } 0 \le r < r_2, \qquad (34)$$

where h is a specified positive constant and T_{amb} is the given surrounding (ambient) temperature. Here h is taken to be 20000 $\text{Wm}^{-2}\text{K}^{-1}$ and T_{amb} to be 300 K.

The problem of interest here is to examine the effect of the thermal superconductor (occupying the region $x^2 + y^2 = r_1^2$, $\ell_1 < z < \ell_2$) on the conduction of heat in the cylindrical system. As before, the surface of the thermal superconductor has a constant temperature to be determined and the total heat flux across that surface is zero.

For this case, the boundary conditions in (8) are not applicable and are replaced by (33) and (34). Thus, the analysis in Section 3 has to be modified to take into consideration the different boundary conditions. The modification is not difficult to carry out. The temperature field $T_2(r, z)$ is still given as written in (10). One may proceed as follows to modify $T_1(r, z)$ and $T_3(r, z)$.

The temperature fields $T_1(r, z)$ and $T_3(r, z)$ in (10) are modified to be given by

$$T_1(r, z) = -\frac{q_0 z}{k_1} + \bar{a}_0 + \sum_{n=1}^{\infty} \bar{a}_n J_0(j_{1,n}\frac{r}{r_2}) \cosh(j_{1,n}\frac{z}{r_2}), \qquad (35)$$

and

$$
\begin{aligned}
T_3(r, z) &= T_{\text{amb}} - \frac{k_3 \bar{d}_0}{r_2 h} + \bar{d}_0 \frac{(z - \ell_3)}{r_2} \\
&\quad + \sum_{n=1}^{\infty} \bar{d}_n J_0(j_{1,n}\frac{r}{r_2}) \\
&\quad \times [\sinh(j_{1,n}\frac{(z - \ell_3)}{r_2}) - \frac{k_3 j_{1,n}}{h r_2} \cosh(j_{1,n}\frac{(z - \ell_3)}{r_2})]. \qquad (36)
\end{aligned}
$$

Subsequently, in the analysis from (11) until (25), one finds that (12), (14), (16), (17), (20), (21), (23) and (24) have to be modified accordingly. Specifically, in (12), (20), a_0 and T_{bottom} are replaced by $-q_0 r_2/k_1$ and $\overline{a}_0$ respectively; $\sinh(j_{1,m}\ell_1/r_2)$ and $\cosh(j_{1,m}\ell_1/r_2)$ in (14) and (21) are interchanged, that is, $\sinh(j_{1,m}\ell_1/r_2)$ and $\cosh(j_{1,m}\ell_1/r_2)$ are superceded by $\cosh(j_{1,m}\ell_1/r_2)$ and $\sinh(j_{1,m}\ell_1/r_2)$ respectively and a_m is replaced by $\overline{a}_m$; in (16) and (23), T_{top} is replaced by $T_{\text{amb}} - k_3\overline{d}_0/(r_2 h)$ and d_0 by $\overline{d}_0$; in (17) and (24), $\sinh(j_{1,m}[\ell_2 - \ell_3]/r_2)$ and $\cosh(j_{1,m}[\ell_2 - \ell_3]/r_2)$ are respectively replaced by $\sinh(j_{1,m}[\ell_2 - \ell_3]/r_2) - k_3 j_{1,m} h^{-1} r_2^{-1} \cosh(j_{1,m}[\ell_2 - \ell_3]/r_2)$ and $\cosh(j_{1,m}[\ell_2 - \ell_3]/r_2) - k_3 j_{1,m} h^{-1} r_2^{-1} \sinh(j_{1,m}[\ell_2 - \ell_3]/r_2)$ and d_m by $\overline{d}_m$.

In setting up the system of linear algebraic equations to determine the unknown coefficients in the representations for T_1, T_2 and T_3, equation (26) is still valid, but (27), (28), (29) and (30) are respectively replaced by

$$
\sum_{n=1}^{N_\infty} \frac{A_{0n}}{r_2^2}[b_n(\cosh(\frac{\sigma_n}{2r_2}[\ell_2 - \ell_1]) + \frac{k_2\ell_1\sigma_n}{k_1 r_2}\sinh(\frac{\sigma_n}{2r_2}[\ell_2 - \ell_1]))
$$
$$
+ c_n(-\sinh(\frac{\sigma_n}{2r_2}[\ell_2 - \ell_1]) - \frac{k_2\ell_1\sigma_n}{k_1 r_2}\cosh(\frac{\sigma_n}{2r_2}[\ell_2 - \ell_1])))]
$$
$$
- \frac{\ell_1 r_1^2}{k_1 r_2^2}\sum_{n=1}^{N_\infty}\frac{f_n}{j_{0,n}}J_1(j_{0,n}) + \frac{1}{2}T_{\text{sc}} - \frac{1}{2}\overline{a}_0
$$
$$
= \quad 0 \ , \tag{37}
$$

$$
\sum_{n=1}^{N_\infty}\frac{A_{mn}}{r_2^2}[b_n\cosh(\frac{\sigma_n}{2r_2}[\ell_2 - \ell_1]) - c_n\sinh(\frac{\sigma_n}{2r_2}[\ell_2 - \ell_1])]
$$
$$
- \sum_{n=1}^{N_\infty}\frac{k_2\sigma_n A_{mn}\cosh(j_{1,m}\ell_1/r_2)}{r_2^2 k_1 j_{1,m}\sinh(j_{1,m}\ell_1/r_2)}
$$
$$
\times[-b_n\sinh(\frac{\sigma_n}{2r_2}[\ell_2 - \ell_1]) + c_n\cosh(\frac{\sigma_n}{2r_2}[\ell_2 - \ell_1])]
$$
$$
- \sum_{n=1}^{N_\infty}\frac{f_n j_{0,n}J_1(j_{0,n})J_0(j_{1,m}r_1/r_2)\cosh(j_{1,m}\ell_1/r_2)}{k_1 j_{1,m}[(j_{0,n}/r_1)^2 - (j_{1,m}/r_2)^2]r_2\sinh(j_{1,m}\ell_1/r_2)}
$$
$$
= \quad 0 \ \text{ for } m = 1, 2, \cdots, 2N_\infty - 1, \tag{38}
$$

16

$$
\sum_{n=1}^{N_\infty} \frac{A_{0n}}{r_2^2} [b_n(\cosh(\frac{\sigma_n}{2r_2}[\ell_2 - \ell_1]) - \frac{(\ell_2 - \ell_3)k_2\sigma_n}{k_3 r_2} \sinh(\frac{\sigma_n}{2r_2}[\ell_2 - \ell_1]))
$$

$$
+ c_n(\sinh(\frac{\sigma_n}{2r_2}[\ell_2 - \ell_1]) - \frac{(\ell_2 - \ell_3)k_2\sigma_n}{k_3 r_2} \cosh(\frac{\sigma_n}{2r_2}[\ell_2 - \ell_1]))]
$$

$$
- \frac{(\ell_2 - \ell_3)r_1^2}{k_3 r_2^2} \sum_{n=1}^{N_\infty} \frac{g_n}{j_{0,n}} J_1(j_{0,n}) + \frac{1}{2}T_{\text{sc}} + \frac{k_3}{2r_2 h}\overline{d}_0
$$

$$
= \frac{1}{2}T_{\text{amb}}, \tag{39}
$$

and

$$
\sum_{n=1}^{N_\infty} \frac{A_{mn}}{r_2^2} [b_n \cosh(\frac{\sigma_n}{2r_2}[\ell_2 - \ell_1]) + c_n \sinh(\frac{\sigma_n}{2r_2}[\ell_2 - \ell_1])]
$$

$$
- \sum_{n=1}^{N_\infty} \frac{k_2\sigma_n A_{mn} B_m}{r_2^2 k_3 j_{1,m}} [b_n \sinh(\frac{\sigma_n}{2r_2}[\ell_2 - \ell_1]) + c_n \cosh(\frac{\sigma_n}{2r_2}[\ell_2 - \ell_1])]
$$

$$
- \sum_{n=1}^{N_\infty} \frac{g_n j_{0,n} J_1(j_{0,n}) J_0(j_{1,m}r_1/r_2) B_m}{k_3 j_{1,m}[(j_{0,n}/r_1)^2 - (j_{1,m}/r_2)^2]r_2}
$$

$$
= 0 \quad \text{for } m = 1, 2, \cdots, 2N_\infty - 1, \tag{40}
$$

where

$$
B_m = \frac{[\sinh(j_{1,m}[\ell_2 - \ell_3]/r_2) - k_3 j_{1,m} h^{-1} r_2^{-1} \cosh(j_{1,m}[\ell_2 - \ell_3]/r_2)]}{[\cosh(j_{1,m}[\ell_2 - \ell_3]/r_2) - k_3 j_{1,m} h^{-1} r_2^{-1} \sinh(j_{1,m}[\ell_2 - \ell_3]/r_2)]}. \tag{41}
$$

Note the presence of two additional unknowns constant $\overline{a}_0$ and $\overline{d}_0$ in (37) and (39). Thus, two more equation are needed to complete the system. These are given by the appropriately modified forms of (12) and (16), that is,

$$
\sum_{n=1}^{N_\infty} \frac{A_{0n}}{r_2^2} [b_n \cosh(\frac{\sigma_n}{2r_2}[\ell_2 - \ell_1]) - c_n \sinh(\frac{\sigma_n}{2r_2}[\ell_2 - \ell_1])] - \frac{1}{2}\overline{a}_0 + \frac{1}{2}T_{\text{sc}}
$$

$$
= -\frac{q_0 \ell_1}{2k_1}, \tag{42}
$$

17

and

$$\sum_{n=1}^{N_\infty} \frac{A_{0n}}{r_2^2}[b_n \cosh(\frac{\sigma_n}{2r_2}[\ell_2 - \ell_1]) + c_n \sinh(\frac{\sigma_n}{2r_2}[\ell_2 - \ell_1])]$$
$$+(\frac{k_3}{2r_2h} - \frac{(\ell_2 - \ell_3)}{2r_2})\bar{d}_0 + \frac{1}{2}T_{sc}$$
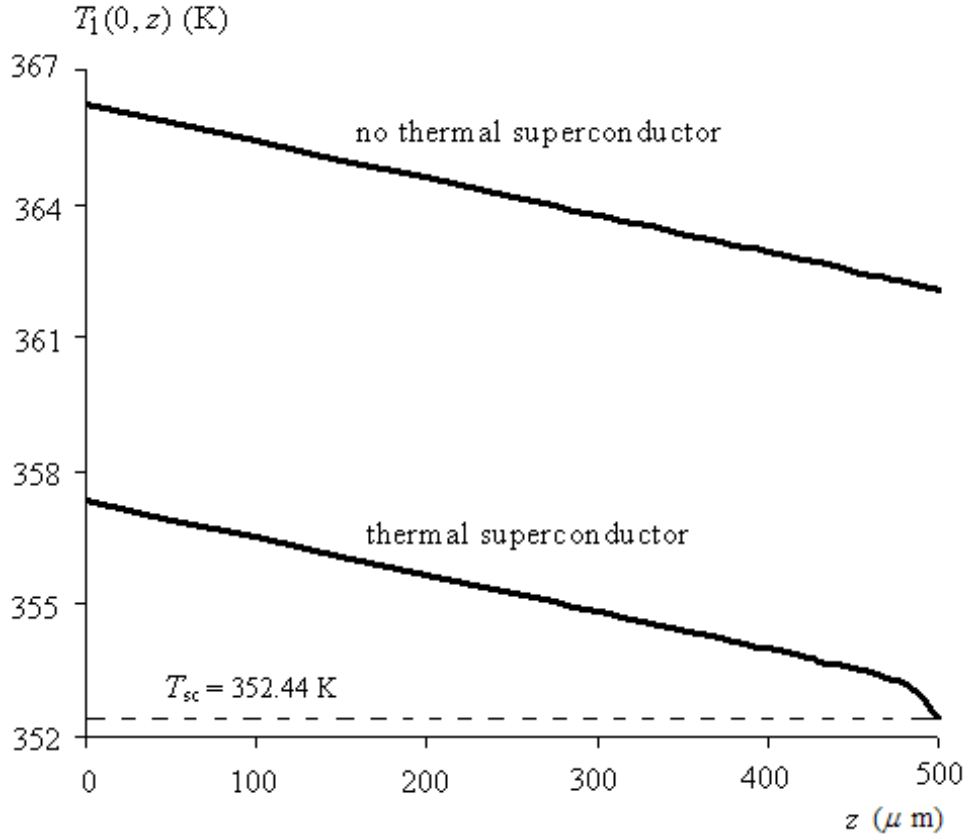$$= \frac{1}{2}T_{amb}. \tag{43}$$

Figure 3. Temperature along the line $r = 0$ in R_1.

18

According to calculation using $N_\infty = 45$, the temperature on the surface of the thermal superconductor is 352.44 K. The presence of the thermal superconductor assists in reducing the overall temperature in R_1. In Figure 3, the temperature along the line $r = 0$ in R_1 (for $0 \le z \le 500$ μm) is compared with the corresponding temperature when there is no thermal superconductor (that is, when the region $x^2 + y^2 < r_2^2$, $\ell_1 < z < \ell_2$) is completely filled with the thermal interface material whose thermal conductivity is $k_2 = 1$ Wm^{-1}K^{-1}). As expected, the graph of temperature $T_1(0, z)$ is almost a straight line which is parallel to the line for the temperature field without the thermal superconductor, except at points where z approaches the value $\ell_1 = 500$ μm (near the thermal superconductor). As z approaches $\ell_1 = 500$ μm, the temperature drops at a more rapid rate to the surface temperature of the thermal superconductor.
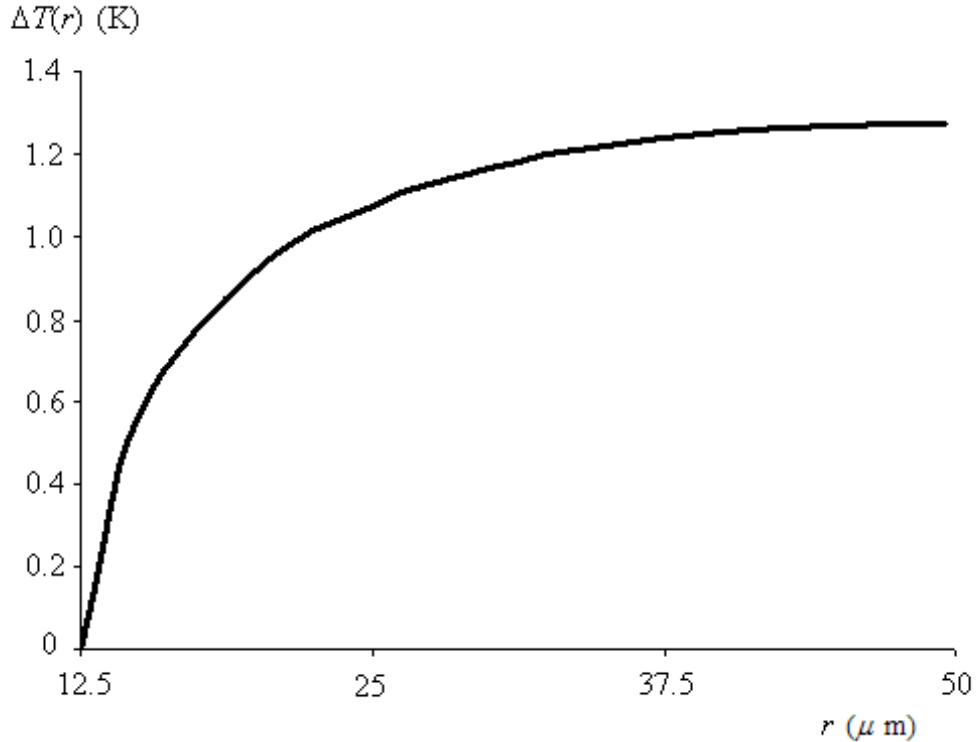

Figure 4. Graph of $\Delta T(r)$ over $12.5 \le r \le 50$ μm.

19

In Figure 4, the temperature change across the thermal interface material, as defined by $\Delta T(r) = T(r, \ell_1) - T(r, \ell_2)$, is plotted against r for $12.5 \le r \le 50$ μm. The temperature change is relatively small with a magnitude of less than 1.28 K, compared to 10 K when the region $x^2 + y^2 < r_2^2$, $\ell_1 < z < \ell_2$ is wholly occupied by the thermal interface material. When there is no thermal superconductor, the temperature changes from 362.08 K on $z = \ell_1 = 500$ μm to 352.08 K on $z = \ell_2 = 510$ μm ($0 \le r \le 50$ μm).

6   Summary

A series solution is obtained for axisymmetric steady-state heat conduction in a multi-material cylindrical system containing a thermal superconductor. The thermal superconductor may be used as a simple model for a carbon nanotube. The truncated series with less than 20 terms is applied to compute the effective thermal conductivity of a representative volume element containing a carbon nanotube. The results obtained are found to be in reasonably good agreement with those calculated using computationally intensive numerical techniques involving several thousand unknowns. The analysis as given in Section 3 for the solution is valid for boundary conditions in which constant temperatures are specified on the top and bottom surfaces of the composite cylinder in Figure 1. Nevertheless, as shown in the second case studies (Section 5), it may be easily modified to include certain other types of boundary conditions.

References

[1] A. Desai, J. Geer and B. Sammakia, Models of steady heat conduction in multiple cylindrical domains, Journal of Electronic Packaging-Transactions of the ASME 128 (2006) 10-17.

[2] S. Berber, Y. K. Kwon and D. Tomanék, Unusually high thermal conductivity of nanotubes, Physical Review Letters 84 (2000) 4613-4616.

[3] P. Hui and H. S. Tan, Temperature distributions in a heat dissipation system using a cylindrical diamond spreader on a copper heat sink, Journal of Applied Physics 75 (1994) 748-757.

[4] S. Iijima, Helical microtubules of graphite carbon, Nature 354 (1991) 56-58.

[5] D. P. Kennedy, Spreading resistance in cylindrical semiconductor devices, Journal of Applied Physics 31 (1960) 1490-1497.

[6] I. V. Singh, M. Tanaka and M. Endo, Thermal analysis of CNT-based nano-composites by element free Galerkin method, Computational Mechanics (2006) (in press). http://dx.doi.org/10.1007/s00466-006-0061-x

[7] J. M. Zhang and Z. H. Yao, Meshless regular hybrid boundary node method, Computer Modeling in Engineering and Sciences 2 (2001) 307-318.

[8] J. M. Zhang, Z. H. Yao and H. Li, A hybrid boundary node method, International Journal for Numerical Methods in Engineering 53 (2002) 751-763.

[9] J. Zhang, M. Tanaka and T. Matsumoto, A simplified approach for heat conduction analysis of CNT-based nano composites, Computer Methods in Applied Mechanics and Engineering 193 (2004) 5597-5609.